Experimental studies on Shear capacity of cementitious RPC Beams using High Strength Reinforcement

Xia Cao[a], Xiao-Fang Deng[b], Ling-Zhi Jin[a], Feng Fu[c*], Kai Qian[a]

Abstract: Reactive Powder Concrete (RPC) is a special concrete where the microstructure is optimized by precise gradation of all particles in the mix to yield maximum density. Therefore, Reactive Powder Concrete exhibits ultra-high strength and durability. The high strength reinforcement (HSR) has high strength and good plastic deformation properties. The combination of RPC and high strength reinforcement can fully exploit their respective advantages. At present, there is little research on shear capacity of HSR reinforced RPC concrete beams, neither are design guidelines for this type of structure. Therefore, it is imperative to make detailed investigations on the shear capacity of this type of concrete. In this paper, thirty-two full scale shear tests of high strength steel reinforced RPC beams were carried out. The parameters affecting the shear capacity of this type of structures were studied, the major failure modes of this type structure due to shear are identified.

Keywords: Beams & girders, Buildings, structures & design, Concrete structures, Reactive Powder Concrete, high strength Reinforcement shear ductility, shear span to depth ratio, reinforcement ratio

1. Introduction

Reactive Powder is an ultra-high strength and high ductility cementitious composite with advanced mechanical properties. It was developed in France in the early 1990s (Aitcin et al,2005). Reactive Powder Concrete (RPC) consists of a special concrete where the microstructure is optimized by precise gradation of all particles in the mix to yield maximum density. It uses extensively the pozzolanic properties of highly refined silica fume and optimization of the Portland cement chemistry to produce the highest strength hydrates. It is

* Corresponding author: E-mail address: cenffu@yahoo.co.uk, ORICD 0000-0002-9176-8159

composed of very fine powders (cement, sand, quartz powder and silica fume), steel fibers (optional) and superplasticizer. The superplasticizer, used at its optimal dosage, decreases the water to cement ratio (w/c) while improving the workability of the concrete. A very dense matrix is achieved by optimizing the granular packing of the dry fine powders (Richard et al.,1995, Dauriac,1997, Basu,1999, Bonneau,2000, Goltermann1997). This compactness gives RPC ultra-high strength and durability. It can achieve compressive strengths ranging from 200 MPa to 800 MPa. This new type of cementitious composite material allows optimization of material use, generation of economic benefits, and provides strong, durable structures.

Nowadays, RPC has been used successfully for buildings and bridges. It is particularly used for isolation and containment of nuclear wastes in Europe due to its excellent impermeability. The requirements for RPC used for the nuclear waste containment structures of Indian Nuclear Power Plants are normal compressive strength, moderate young's modulus value, uniform density, good workability, and high durability.

It is widely known that the high strength reinforcement has high strength and good plastic deformation properties. The combination of RPC and high strength reinforcement can fully exploit their respective advantages. At present, there are few researches on shear capacity of RPC concrete beams using high strength reinforcement, neither are design guidelines for this type of structure. Therefore, the pertinent research is imperative.

The research on Reactive Powder Concrete has attracted great interest recently. Su et al (2019) made investigation on mode I fracture features of steel fiber-reinforced reactive powder concrete using semi-circular bend test. He et al. (2018) studied the Experimental evaluation of shear connectors using reactive powder concrete under natural curing condition. Ruan et al (2018) studied the Mechanical behaviors of nano-zirconia reinforced reactive powder concrete under compression and flexure. Hou et al. (2017) Evaluation of residual mechanical properties of steel fiber-reinforced reactive powder concrete after exposure to high temperature using nondestructive testing. Wang et al. (2019) studied on the axial compressive behavior of reactive powder concrete-filled circular steel tube stub columns. Yu et al. (2018) made experimental investigation of CFRP confined hollow core Reactive Powder Concrete columns.

The research on the shear behavior of RPC concrete is still limited. In 2018, 18 tests have been done by Ridha, et al. (2018) to investigate the Shear Strength of Reactive Powder

Concrete Beams. Voo et al (2006,2010) performed shear failure tests on prestressed RPC beams and analyzed the shear capacity of RPC beams without web reinforcement based on plasticity theory. The test parameters were shear span-to-effective depth ratio and steel fibre dosage. They also developed calculation model for shear capacity. In 2015,72 pull out tests have been performed by Deng et al (2015) from Beijing University of Technology on RPC concrete structure. They studied the influence of different factors on the bonding performance and established the calculation formula of the anchorage length of high-strength steel in RPC. In addition, 12 shearing tests of RPC beams were also performed with different parameters, and the plastic shear coefficient is introduced based on plastic theory to develop the calculation formula for the shear resistance. Xu et al (2014) carried out the shear performance test of 9 high-strength steel RPC beams with different factors and concluded that the shear capacity increased with the increase of the close stirrup ratio. The prestress force can significantly improve the shear capacity of the beam. The empirical formula for the shear capacity of ultra-high performance concrete beams is established. Sun et al. (2016) carried out the pull-out test of cubic specimens to study the bond stress-slip process and failure mode of high-strength steel RPC components, and analysed the influence of various factors on the bond performance and developed the formula for calculating the ultimate bond stress and critical anchor length. Jin et al. (2015) performed flexural test of high-strength steel RPC beams, analyse the crack development patterns. The applicability of the current Chinese concrete code on high-strength steel RPC beams designed was verified. The calculation method of the ultimate flexural capacity of this type of beams was proposed based on the test results.

From above literature review, it can be seen that, although there is some research on RPC beams, but none research on the shear capacity of cementitious composite reactive powder concrete beams using high strength reinforcement is available. Therefore, in this paper, 32 full scale shear tests of high strength reinforced RPC beams were carried out. The parameters affecting the behaviour of this type of structures have been studied in detail, relevant design recommendations have also been made. A companion paper to develop the calculation methods for the shear capacity of this type of structure will be presented separately.

2. Experimental program

32 full scale tests were performed to investigate the shear capacities of this new type of beams. The main compositions of RPC beams are high strength steel bars HRB500, HRB400 and HRB300 with reactive powder concrete. The effect of the shear span to effective depth

ratio, the ratio of longitudinal rebars, stirrup ratio, ratio of web reinforcement, dosage of the steel fibre, the section shape and the angle of the shear stirrup configuration to HSR reinforced RPC concrete were studied based on the test results. Due to the vast numbers of the tests, only the typical tests are demonstrated here.

2.1 Test specimens and Test Material

All the beams' spans are 2200mm, with the inflexion span of 1800 mm. The longitudinal bars were Chinese high strength steel HRB500 with HRB 400 as shear link. HPB300 is the lace bar. As it is shown in Li (2010) the maximum steel ratio of RPC beam can be 10%, therefore, to ensure shear failure, large number of longitudinal bars were used, as it is shown in Table 1. The detailing of the reinforcement for the tested beams is shown in Figure 1

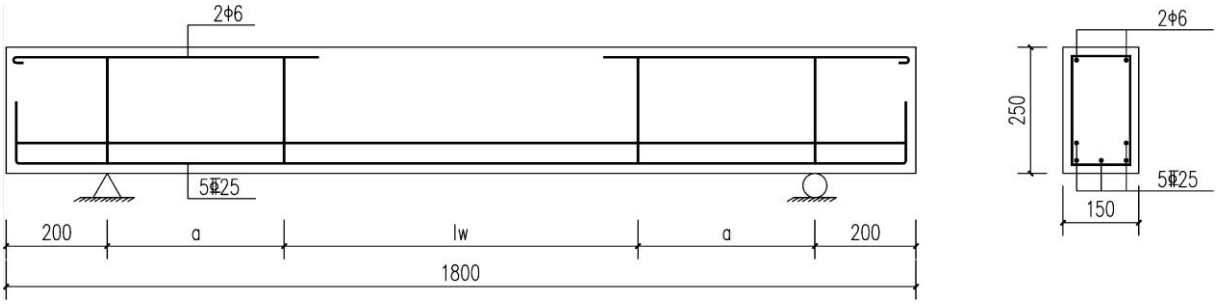

(a) Detailing of Concrete Reinforcement of rectangular beam without web reinforcement

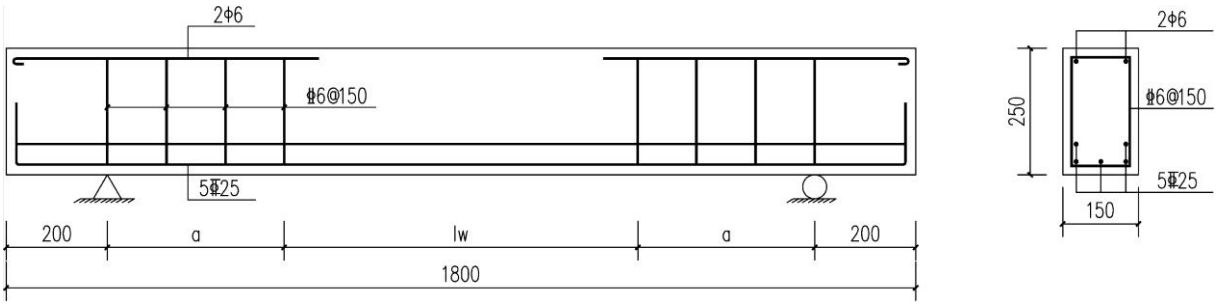

(b) Detailing of Concrete Reinforcement of rectangular beam with web reinforcement

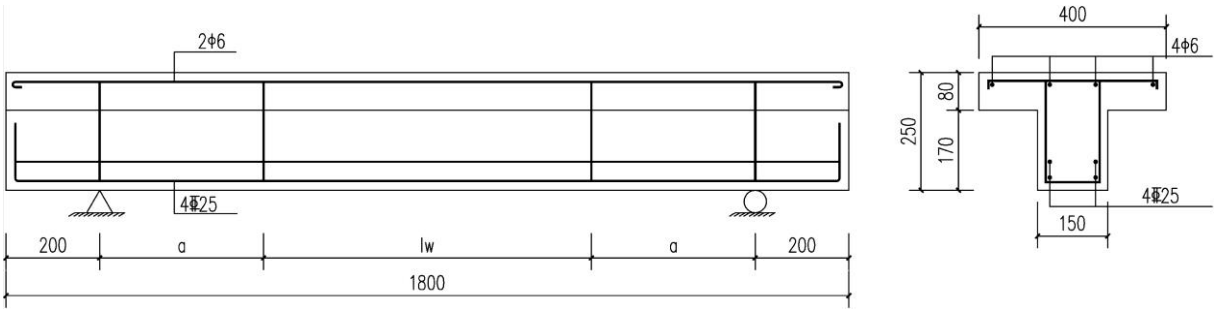

(c) Detailing of Concrete Reinforcement of T beam without web reinforcement

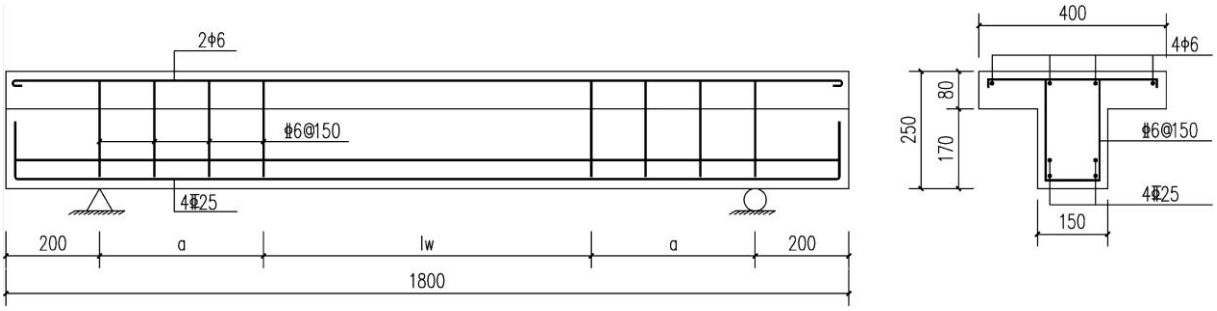

(d) Detailing of Concrete Reinforcement of T beam with web reinforcement

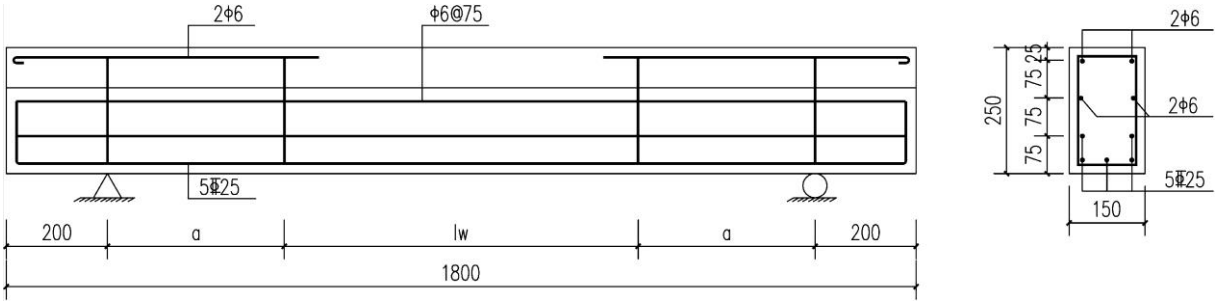

(e) Detailing of Concrete Reinforcement of rectangular beam with double web reinforcement

Figure 1 RC detailing of the testing beams

Table 1 The key parameter of the testing beams

	λ	Longitudinal rebar	ρ_s/%	stirrup	ρ_{sv}/%	web reinforcement	ρ_{sh}/%	ρ_f/%	Shape of the cross-section	θ_{sv}/°
LL1	2.25	4D25	6.58	-	0	-	0	2	R	-
LL2	2.25	4D25	6.58	C6@225	0.17	-	0	2	R	90°
LL3	2.25	4D25	6.58	C6@150	0.25	-	0	2	R	90°
LL4	2.25	4D25	6.58	C6@65	0.58	-	0	2	R	90°
LP1	2.25	3D25	4.48	-	0	-	0	2	R	-
LP2	2.25	5D25	8.18	-	0	-	0	2	R	-
LH1	1.5	4D25	6.58	-	0	-	0	2	R	-
LH2	3	4D25	6.58	-	0	-	0	2	R	-
LR1	2.25	4D25	6.58	-	0	-	0	-	R	-
LR2	2.25	4D25	6.58	-	0	-	0	1	R	-
LR3	2.25	4D25	6.58	-	0	-	0	3	R	-
LZ1	1	5D25	8.18	-	0	-	0	2	R	-
LZ2	2.25	5D25	8.18	-	0	-	0	2	R	-

	λ	Longitudinal rebar	ρ_s/%	stirrup	ρ_{sv}/%	web reinforcement	ρ_{sh}/%	ρ_f/%	Shape of the cross-section	θ_{sv}/°
LZ3	3.5	5D25	8.18	-	0	-	0	2	R	-
LZ4	1.5	5D25	8.18	C6@150	0.25	-	0	2	R	90°
LZ5	2.25	5D25	8.18	C6@150	0.25	-	0	2	R	90°
LZ6	3	5D25	8.18	C6@150	0.25	-	0	2	R	90°
LC1	2.25	5D25	8.18	C6@75	0.50	-	0	2	R	90°
LC2	3	5D25	8.18	C6@300	0.13	-	0	2	R	90°
LC3	3	5D25	8.18	C6@100	0.38	-	0	2	R	90°
LY1	3.5	5D25	8.18	-	0	-	0	2	T	-
LY2	2.25	5D25	8.18	-	0	-	0	2	T	-
LY3	2.25	5D25	8.18	C6@150	0.25	-	0	2	T	90°
LT1	1.5	4D25	6.58	C6@150	0.25	-	0	2	R	90°
LT2	1.5	6D25	9.87	C6@150	0.25	-	0	2	R	90°
LT3	2.25	6D25	9.87	C6@150	0.25	-	0	2	R	90°
LW1	2.25	5D25	8.18	-	0	C6@75	0.25	2	R	-
LW2	2.25	5D25	8.18	-	0	C6@75	0.51	2	R	-
LW3	2.25	5D25	8.18	-	0	C6@50	0.76	2	R	-
LM1	2.25	5D25	8.18	C6@150	0.25	-	0	2	R	75°
LM2	2.25	5D25	8.18	C6@150	0.25	-	0	2	R	60°
LM3	2.25	5D25	8.18	C6@150	0.25	-	0	2	R	45°

2.2 Test Rigs

Figure 2 Test Rigs

As it is shown in Figure 2., 4-point bending tests were conducted. A 200-t hydraulic jack was used for the test. The beam was pin supported at two ends. The load was applied incrementally, with 5-10 minutes interval at every loading step. The crack, deflection and strain were recorded using various instrumentations and data logger. Before cracking was noticed, the load increment was 20kN. When diagonal cracks occurred, the increment changed to 50 KN. When the load reached 90% of the ultimate load, 30 KN load increment was used until the failure of the beams.

3. Experimental results and analysis

Based on the test results, the shear capacity of this type of beams is investigated. Considering large number of specimens, during the tests, the specimens are divided into certain groups according to different influence parameters.

Three types of failure are observed during the test:

(1) Diagonal tension failure

Failure often occurs when the shear span ratio of the beams without web reinforcement is large ($\lambda>3$) or less stirrups with web reinforcement are used. Once the diagonal crack appears, it develops rapidly, and the stirrups between the cracks yield and break suddenly, which has obvious brittle failure noticed. When the concrete is damaged, the number of cracks is small and the crack width is wide, and the main diagonal cracks are evident. The bearing capacity depends on the tensile strength of concrete, and the cracking load are close to the ultimate load.

(2) Shear-compression failure

Failure often occurs in beams with web reinforcement with medium shear-span ratio (range of λ is 1.5-3) and moderate stirrup ratio. The diagonal crack develops slowly with the load. The widest diagonal crack develops into critical diagonal crack, and the stirrup yields. Finally, the concrete in the shear-compression zone is crushed, which has a certain ductility. When the beam is damaged, there are many main inclined cracks with uniform distribution.

(3) Diagonal compression failure

Failure occurs when the shear span ratio is small ($\lambda< 1.5$) and the more stirrups are arranged. The diagonal cracks form a crack zone from loading point to support. The concrete is crushed and destroyed, and the stirrups are not yielded at ultimate load, indicating brittle failure.

3.1 Effect of Shear span to effective depth ratio

3.1.1 Beam without web reinforcement

3.1.1.1 Shear capacity

As it shown in Table 2, Figure 3 and Figure 4, the shear capacity of testing beams decreases with the increase of shear span to effective depth ratio. When the shear span ratio increases from 1 and 1.5 to 2.25, the shear capacity decreases rapidly for beams with longitudinal bar ratio of 65.1% and 45.8% respectively. When the shear span to depth ratio increases from 2.25 to 3.5, the shear capacity decreases slowly, by 5.9% and 33.0% respectively, and the impact of the increase of shear span ratio on shear capacity has become smaller.

3.1.1.2 Failure mode

It can be seen that the change of shear span to depth ratio greatly affects the failure mode for beams without web reinforcement. For LZ1, the cracks are small, and only one main diagonal crack is formed, so it is diagonal compression failure, which is between the loading point and support. Although the failure of LH1 with λ of 1.5 is caused by the major diagonal cracks at the right end, there are small cracks around it. Its failure pattern is between shear-compression failure and diagonal compression failure, but it is closer to the latter. For the testing beams with λ of 2.25 and 3.5, cracks developed rapidly, and their cracking loads and ultimate loads are similar to those of other test beams, and diagonal tension failure occurs. For LL1 and LZ2, cracks are developed from one or two primary cracks until a critical crack is formed and shear-compression failure occurs.

(a)LH1（λ=1.5，ρ_s=6.58%）

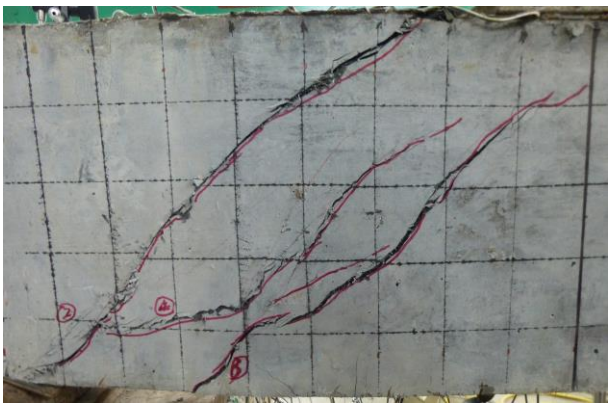

(b)LL1（λ=2.25，ρ_s=6.58%）

(c)LH2（λ=3，ρ_s=6.58%）

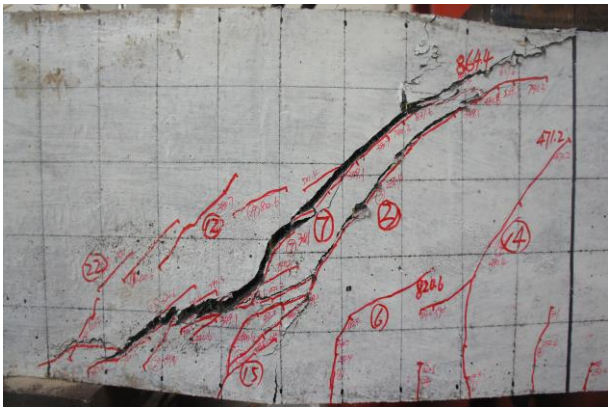

(d)LZ2（λ=2.25，ρ_s=8.18%）

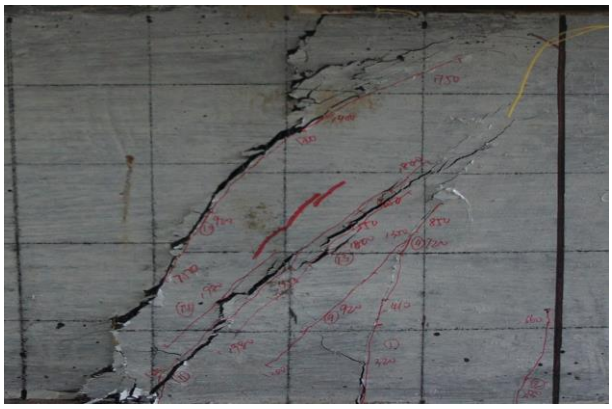

(e)LZ1（λ=1，ρ_s=8.18%）

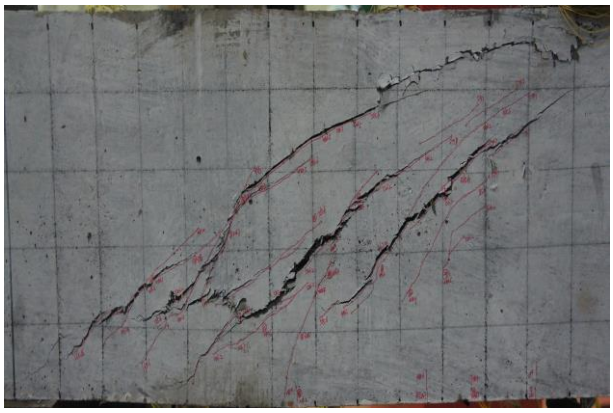

(f) LZ3（λ=3.5，ρ_s=8.18%）

Figure 3 Failure mode of beam under shear

Table 2 Test results for RPC beams

Test	λ	ρ_s/%	P_{cr}/kN	P_u/kN	w_{cr}/mm	w_u/mm	θ_w/°	Failure pattern
LH1	1.5	6.58	202	1313	0.02	4.2	45	Diagonal compression
LL1	2.25	6.58	220	712	0.01	2.2	45	Shear-compression
LH2	3	6.58	241	670	0.02	3.5	38	Diagonal Tension
LZ1	1	8.18	720	2584.6	0.015	1.2	56	Diagonal compression
LZ2	2.25	8.18	250.4	901	0.05	10	37	Shear-compression
LZ3	3.5	8.18	299	604.1	0.02	5	29	Diagonal Tension

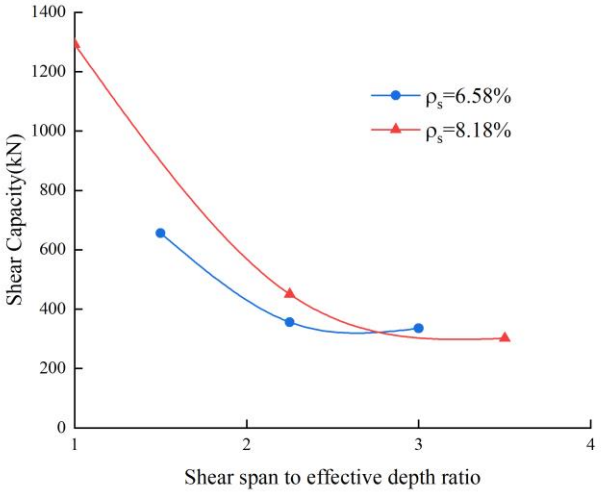

Figure 4 Relationship of shear capacity V.S. shear span to depth ratio

3.1.2 Beam with web reinforcement

3.1.2.1 Shear capacity

As it shown in Table 3, Figure 5 and Figure 6, the shear capacity of test beams decreases with the increase of shear span to effective depth ratio. When the shear span ratio increases from 1.5 to 2.25, the shear capacity of the three groups of test beams decreases by 26.35%, 26.18% and 32.53%, respectively. It can be seen that the influence of shear span ratio on the shear capacity of the beams with web reinforcement is less than that of the beams without web reinforcement, but it still plays an important role.

3.1.2.2 Failure mode

As shown in figs. 5 and table 3, compared with the beams without web reinforcement, the beams with web reinforcement having a shear span ratio of 1.5 (LT1, LZ4, LT2) no longer suffer from diagonal compression failure and are transformed into shear-compression failure due to the role of stirrups. Flexural shear failure occurred in LZ6 with large shear span. The maximum crack caused by the ultimate failure of LZ6 is no longer located in the shear span region but tends to another loading point from one loading point. The strain gauge data acquisition system can tell that most of the stirrups in the shear span region have yielded, and the longitudinal bars in the middle span have reached the yield strength, which has the mode of shear failure and bending failure. The shear-span ratios of the other test beams are moderate, and shear-compression failure occurs.

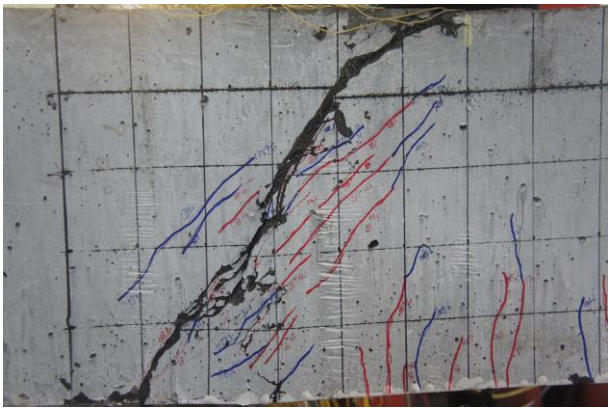

(a) LT1（λ=1.5，ρ_s=6.58%）

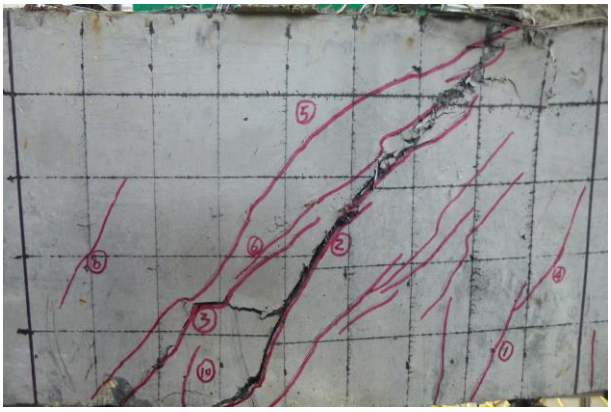

(b) LL3（λ=2.25，ρ_s=6.58%）

(c)LZ4（λ=1.5，ρs=8.18%）

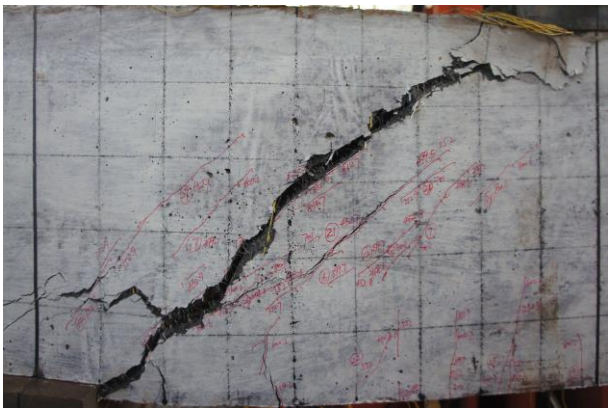

(d) LZ5（λ=2.25，ρs=8.18%）

(e) LZ6（λ=3，ρ_s=8.18%）

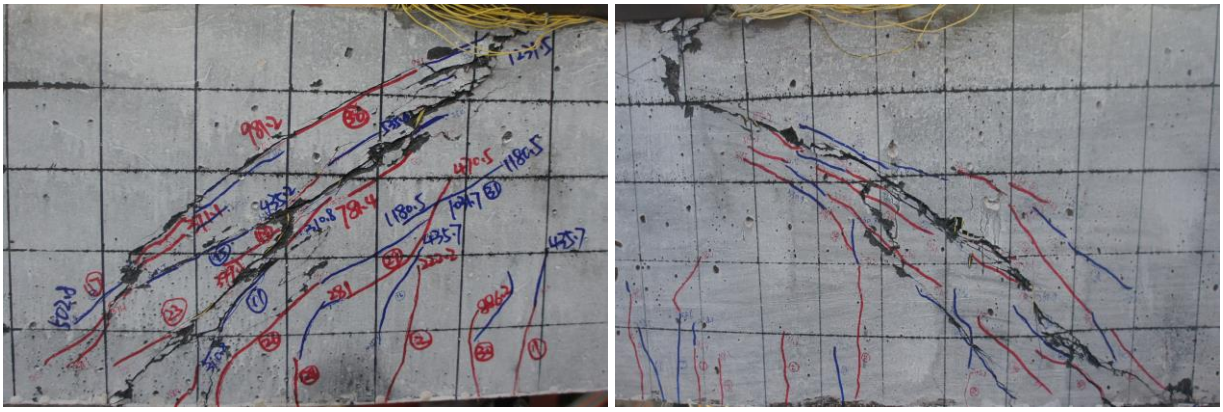

(f) LT2（λ=1.5，ρ_s=9.87%）　　(g) LT3（λ=2.25，ρs=9.87%）

Figure 5 Failure mode of beams under shear

Table 3 Test results for RPC beams

	λ	ρ_s/%	P_{cr}/kN	P_u/kN	w_{cr}/mm	w_u/mm	θ_w/°	Failure pattern
LT1	1.5	6.58	170.3	1170.0	0.02	22.00	45	Shear-compression
LL3	2.25	6.58	200.5	861.7	0.04	7.0	43	Shear-compression
LZ4	1.5	8.18	200.6	1362.3	0.01	14.00	43.8	Shear-compression
LZ5	2.25	8.18	250.8	1005.6	0.02	1.55	37	Shear-compression
LZ6	3	8.18	338.4	836.6	0.06	0.72	45	Flexural shear failure
LT2	1.5	9.87	251.1	1548.8	0.01	1.05	40	Shear-compression
LT3	2.25	9.87	181.1	1045.0	0.01	2.00	35	Shear-compression

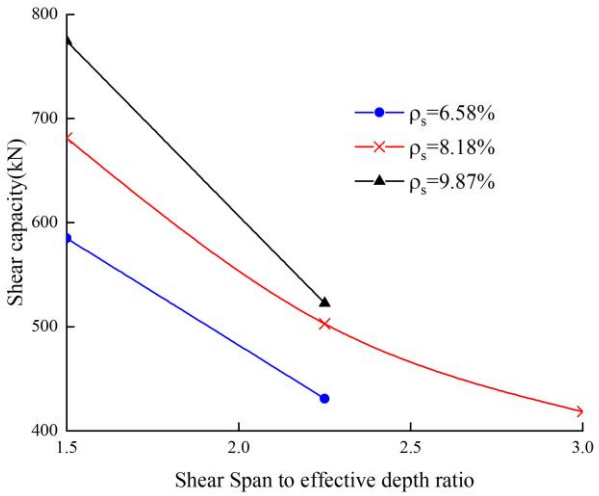

Figure 6 Relationship of shear capacity V.S. shear span to depth ratio

3.2 Effect of Longitudinal rebar ratio

3.2.1 Beam without web reinforcement

3.2.1.1 Shear capacity

As it shown in Table 4, Figure 7 and Figure 8, the shear capacity of beams without web reinforcement increases with the increase of longitudinal reinforcement ratio. The longitudinal reinforcement ratio increased from 4.48% to 6.58% (the longitudinal reinforcement ratio increased by 46.9%) and the shear capacity increased by 56.2%, from 6.58% to 8.18% (the longitudinal reinforcement ratio increased by 24.3%) and the shear capacity increased by 26.5%. It can be seen that the relationship between longitudinal reinforcement ratio and shear capacity tends to be linear.

3.2.1.2 Failure mode

From the test results, we can conclude that the increase of longitudinal reinforcement ratio has little effect on the failure mode of the beams without web reinforcement. LP1, LL1 and LZ2 are all shear-compression failure. The cracks develop slowly and are all developed by a primary inclined crack, and ultimately connect the loading point and the support to form a critical crack.

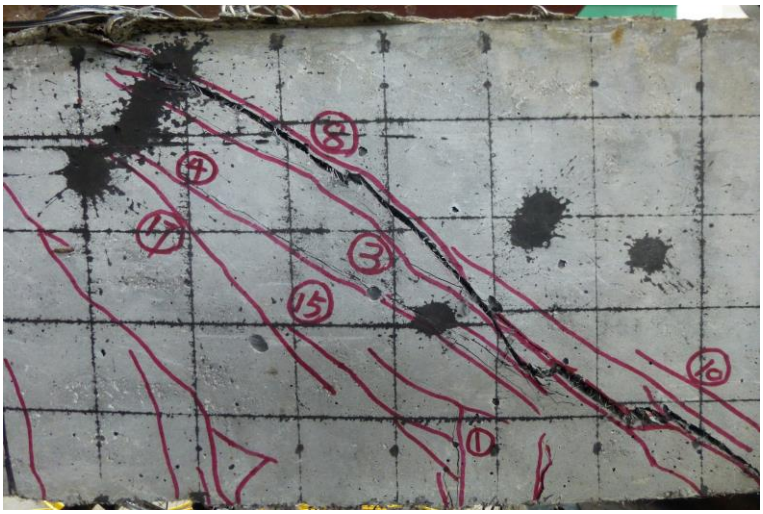

Figure 7 LP1（λ=2.25，ρ_s=4.48%）

Table 4 Test results for RPC beams

ρ_s/%	λ	P_{cr}/kN	P_u/kN	w_{cr}/mm	w_u/mm	θ_w/°	Failure mode

	ρ_s/%	λ	P_{cr}/kN	P_u/kN	w_{cr}/mm	w_u/mm	θ_w/°	Failure mode
LP1	4.48	2.25	140.8	601	0.06	3	40	Shear-compression
LL1	6.58	2.25	220	712	0.01	2.2	45	Shear-compression
LZ2	8.18	2.25	250.4	901	0.05	10	37	Shear-compression

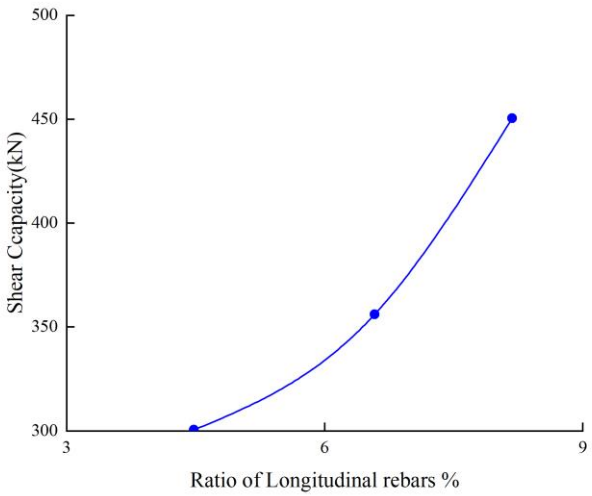

Figure 8 Shear Capacity V.S. Ratio of Longitudinal rebars

3.2.2 Beam with web reinforcement

3.2.2.1 Shear capacity

The test results from table 5 and figure 10, the shear span ratio of LL3, LZ5 and LT3 is 2.25. When the longitudinal reinforcement ratio is increased from 6.58% to 8.18% (the longitudinal reinforcement ratio is increased by 53.4%), the shear capacity is increased by 16.7%. When the longitudinal reinforcement ratio is increased from 8.18% to 9.87% (the longitudinal reinforcement ratio is increased by 20.6%), the bearing capacity is increased by 3.9%. Similarly, when the ratio of longitudinal reinforcement increases from 6.58% to 8.18%, the shear capacity of test beams with 1.5 shear span ratio increases by 16.4%, and 13.7% when the ratio of longitudinal reinforcement increases from 8.18% to 9.87%.

3.2.2.2 Failure mode

The test results also show that the main diagonal cracks of the test beam are clearly visible, and the loading points and supports are connected. The stirrups between the cracks yield, and the failure modes are shear-compression failure. At the same time, it is not difficult to see that the longitudinal reinforcement ratio has a certain impact on the failure mode of the beam with web reinforcement. Among them, LT2 and LT3 have higher longitudinal reinforcement

ratio, and RPC is crushed and fallen off at the belly of the beam. LT2 has formed a wider diagonal crack zone, so the failure mode is that RPC is crushed and sheared, that is to say, the failure of the beam has a certain nature of diagonal compression failure.

Table 5 Test results for RPC beams

	ρ_s/%	λ	P_{cr}/kN	P_u/kN	w_{cr}/mm	w_u/mm	θ_w/°	Failure mode
LL3	6.58	2.25	200.5	861.7	0.04	7.0	43	Shear-compression
LZ5	8.18	2.25	250.8	1005.6	0.02	1.55	37	Shear-compression
LT3	9.87	2.25	181.1	1045.0	0.01	2.00	35	Shear-compression
LT1	6.58	1.5	170.3	1170.0	0.02	22.00	45	Shear-compression
LZ4	8.18	1.5	200.6	1362.3	0.01	14.00	43.8	Shear-compression
LT2	9.87	1.5	251.1	1548.8	0.01	1.05	40	Shear-compression

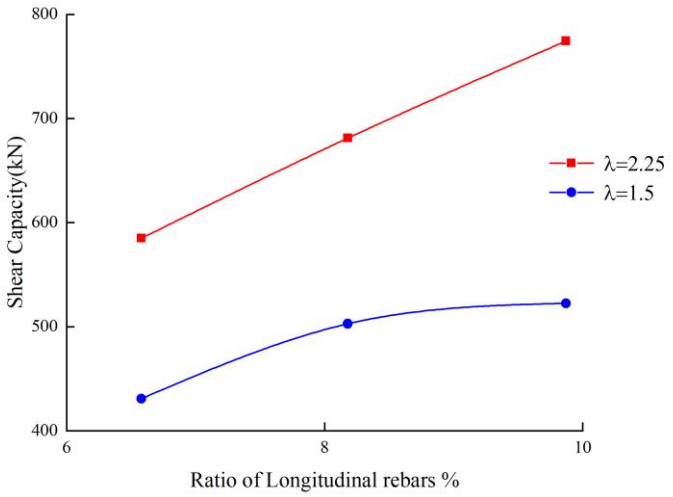

Figure 9 Shear Capacity V.S. Ratio of Longitudinal rebars

3.3 Effect of Stirrup bar ratio

The test results and failure modes are shown in Figure 10 and Table 6.

3.3.1 Failure mode

From Figure 10 and table 6, it can be seen that the failure modes change with the increase of stirrup ratio: when the shear span ratio is moderate, the longitudinal reinforcement ratio is

small but the stirrup ratio is large (LL4), the cracks in inclined section are fine and dense, and the bending failure of the normal section of the test beam takes precedence over the shear failure of the inclined section, and the bending failure of the test beam is bending failure. When the shear span ratio is large and the longitudinal reinforcement ratio is suitable, the test beam will no longer suffer from cable-stayed failure but will be transformed into shear-compression failure (LC2). Continuously increasing the stirrup ratio, the failure mode changed from shear-compression failure to bending-shear failure (LZ6 and LC3). Therefore, the ratio of stirrups improves the failure mode of RPC beams obviously.

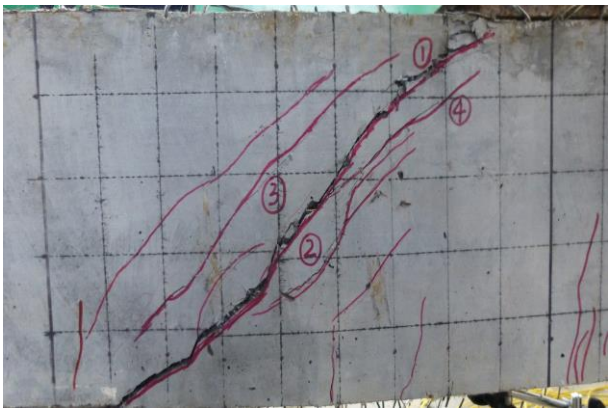

(a) LC1 (ρ_{sv}=0.70%,ρ_s=8.18%,λ=2.25)

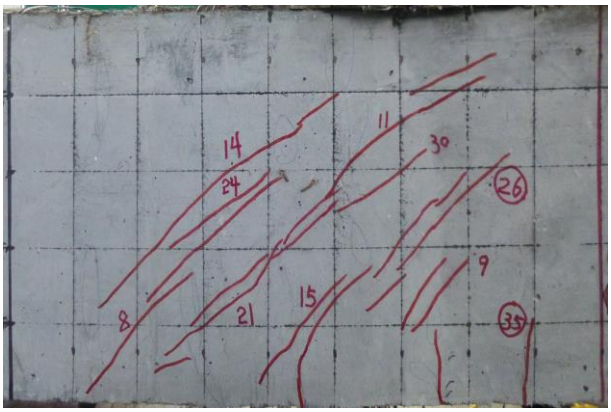

(b) LL4 (ρ_{sv}=0.58%,ρ_s=6.58%,λ=2.25)

(c) LC1 (ρ_{sv}=0.50%,ρ_s=8.18%,λ=2.25)

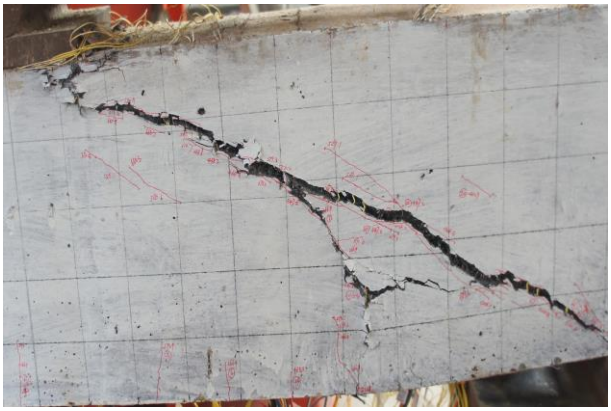

(d)LC2 (ρ_{sv}=0.13%, ρ_s=8.18%,λ=3)

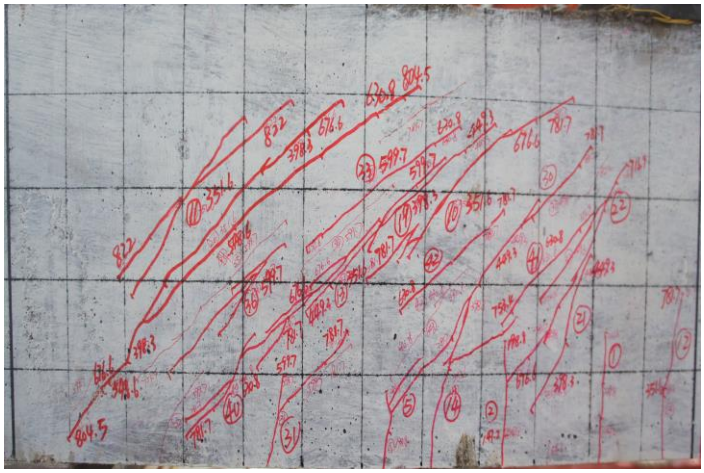

(e)LC3 (ρ_{sv}=0.38%,ρ_s=8.18%,λ=3)

Figure 10 Failure mode of RPC beams

Table 6 Test results for RPC beams

	ρ_{sv}/%	ρ_s/%	λ	P_{cr}/kN	P_u/kN	w_{cr}/mm	w_u/mm	θ_w/°	Failure mode
LL1	0	6.58	2.25	220	712	0.01	2.2	45	Shear-compression
LL2	0.17	6.58	2.25	201.4	838.5	0.02	3	45	Shear-compression
LL3	0.25	6.58	2.25	200.5	861.7	0.04	7.0	43	Shear-compression
LL4	0.58	6.58	2.25	200.5	852.5	0.02	0.32	45	Flexural failure
LZ2	0	8.18	2.25	250.4	901	0.05	10	37	Shear-compression
LZ5	0.25	8.18	2.25	250.8	1005.6	0.02	1.55	37	Shear-compression
LC1	0.50	8.18	2.25	259.7	1058.4	0.02	10	42.5	Shear-compression
LC2	0.13	8.18	3	266.9	709.3	0.04	10	36	Shear-compression
LZ6	0.25	8.18	3	338.4	836.6	0.06	0.72	45	Flexural shear
LC3	0.38	8.18	3	319.9	843.4	0.02	0.34	37	Flexural shear

3.3.2 Shear capacity

When the shear span ratio is 2.25 and the reinforcement ratio is 6.58%, the shear bearing capacity increases dramatically at first, then tends to be flat or even decreases with the increase of the stirrup ratio: the stirrup ratio increases from 0 to 0.17%, the shear bearing

capacity increases by 17.8%; the shear bearing capacity increases by 2.8% from 0.17% to 0.25%; and the shear bearing capacity decreases when the stirrup ratio increases from 0.25% to 0.58%. 1.1%. When the shear span ratio remains unchanged and the reinforcement ratio increases to 8.18%, the shear capacity increases linearly: the stirrup ratio increases from 0 to 0.25%, the shear capacity increases by 11.6%, and the shear capacity increases by 5.3% when the shear span ratio increases from 0.25% to 0.50%. When the reinforcement ratio is 8.18%, the shear bearing capacity decreases as a whole when the shear span ratio increases from 2.25 to 3, and the relationship with the stirrup ratio changes again to that with the increase of stirrup ratio, the shear bearing capacity increases dramatically at first, then slowly: the stirrup ratio increases from 0.13 to 0.25%, and the shear bearing capacity increases by 17.9%; when the stirrup ratio increases from 0.25% to 0.38%, the shear bearing capacity increases. The force was reduced by 0.8%. With the increase of shear span ratio, the development of shear capacity returns to the trend of reinforcement ratio when it is small.

3.4 Effect of Ratio of web horizontal reinforcement

The test results and failure modes are shown in Figure 11 and Table 7.

3.4.1 Failure mode

It can be seen that, the ratio of horizontal web reinforcement has little influence on the failure mode of test beams. All three test beams with web reinforcement have a clear and visible critical crack developed from the initial main diagonal crack, so they are all shear-compression failure. However, with the increase of the ratio of horizontal web reinforcement, the crack develops fully, and the inclination angle increases.

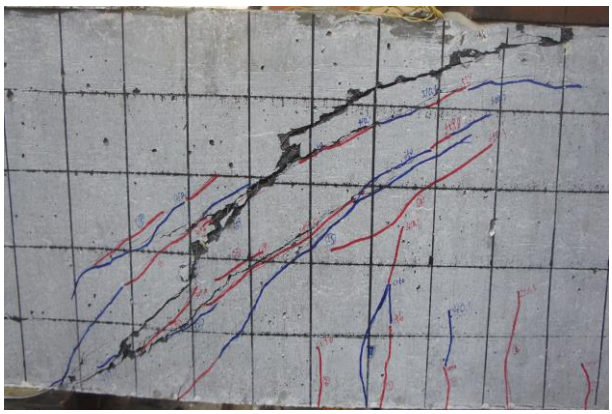

(a) LW1 (ρ_{sh}=0.25%)

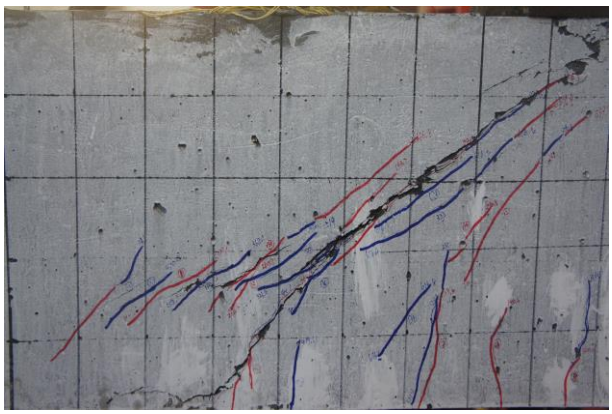

(a)LW2 (ρ_{sh}=0.51%)

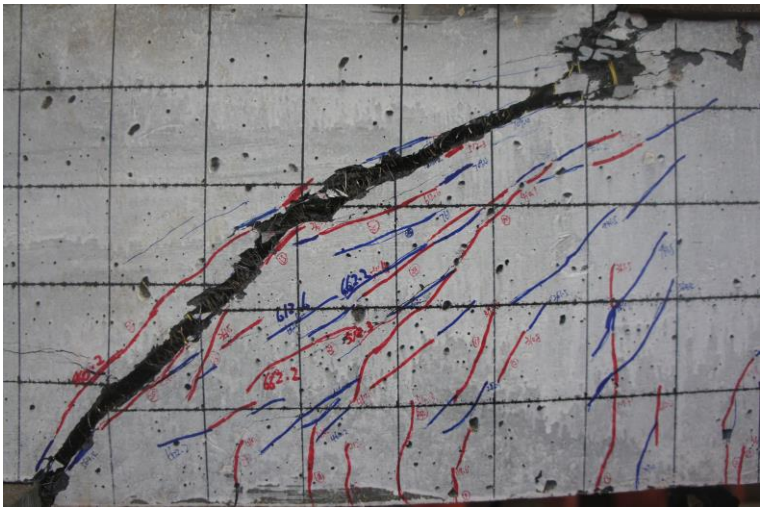

(c)LW3 (ρ_{sh}=0.76%)

Figure 11 Failure mode of RPC beams

Table 7 Test results for RPC beams

	ρ_{sh}/%	ρ_{sv}/%	P_{cr}/kN	P_u/kN	w_{cr}/mm	w_u/mm	θ_w/°	Failure mode
LZ5	0	0.25	250.8	1005.6	0.02	1.55	37	Shear-compression
LC1	0	0.50	259.7	1058.4	0.02	10	42.5	Shear-compression
LW1	0.25	0	189.7	750	0.01	1.07	45	Shear-compression
LW2	0.51	0	260.9	893	0.02	1.2	45	Shear-compression
LW3	0.76	0	212.1	968	0.01	2.42	60	Shear-compression

3.4.2 Shear capacity

When the ratio increases from 0.25% to 0.50%, the shear capacity increases by 5.3%. Under the same conditions, when the ratio of horizontal web reinforcement increases from 0.25% to 0.51%, the shear capacity increases by 19.1%, from 0.51% to 0.76%, and the shear capacity increases by 8.4%. It can be seen that increasing the ratio of horizontal web reinforcement can improve the shear capacity of the beam. When the reinforcement ratio is the same, it can be seen that the horizontal web reinforcement ratio is far less effective than the stirrup ratio in shear capacity.

3.5 Effect of Dosage of steel fiber

The test results and failure modes are shown in Figure 12 and Table 8.

3.5.1 Failure mode

The failure modes of the test beams are improved by adding steel fibers: LR1 without steel fibers has fewer oblique cracks in the shear span, the main diagonal cracks develop rapidly, the cracking load and the failure load are very close, and the test beams are cable-stayed failure. Due to the steel fibers, the development of RPC cracks is delayed, the tensile and compressive properties are improved, and a main oblique crack is clearly visible in the oblique crack zone. The ultimate failure mode of RPC is changed from cable-stayed failure to shear-compressive failure.

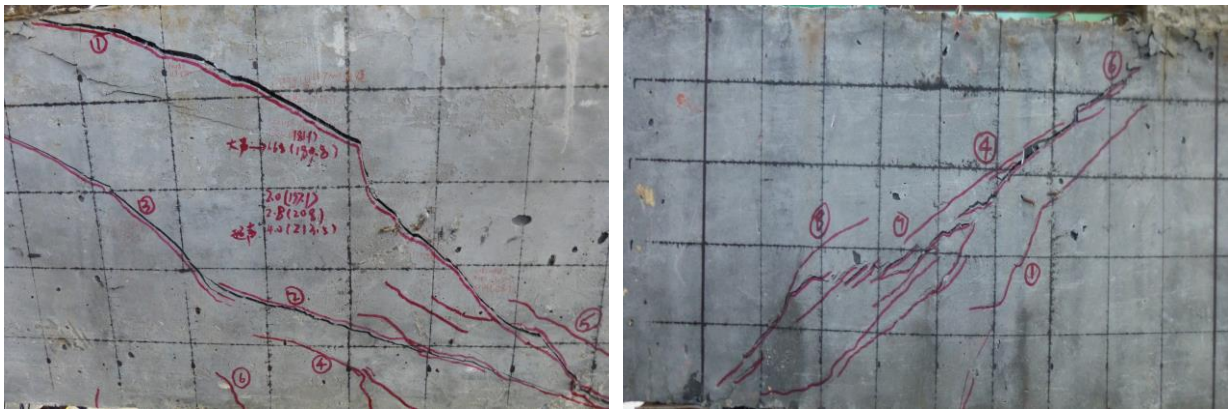

(a) LR1（ρ_{sh}=0%）　　(b) LR2（ρ_{sh}=1%）

(c) LR3（ρ_{sh}=3%）

Figure 12 Failure mode of RPC beams

Table 8 Test results for RPC beams

	ρ_f/%	P_{cr}/kN	P_u/kN	w_{cr}/mm	w_u/mm	θ_w/°	Failure mode
LR1	0	81.7	232.5	0.04	4	45	Diagonal Tension
LR2	1	151.5	499.5	0.04	1.4	45	Diagonal Compression

	ρ_f/%	P_{cr}/kN	P_u/kN	w_{cr}/mm	w_u/mm	θ_w/°	Failure mode
LL1	2	220	712	0.01	2.2	45	Diagonal Compression
LR3	3	251.4	831	0.02	8	44	Diagonal Compression

3.5.2 Shear capacity

When the volume ratio of steel fibers increases from 0 to 1%, the shear capacity increases by 114.8%; when the volume ratio of steel fibers increases from 1% to 2%, the shear capacity increases by 42.5%; when the volume ratio of steel fibers increases from 2% to 3%, the shear capacity increases by 16.7%, and the increase is obviously smaller. Therefore, when the volume ratio of steel fibers is 2%, the shear capacity can be improved greatly.

3.6 Effect of Shape of the section

The test results and failure modes are shown in Figure 13 and Table 9.

3.6.1 Failure mode

The change of section shape makes the failure mode of LZ3 beams without web bar change from cable-stayed failure to shear-compression failure. The change of LZ 2 and LZ5 which were originally shear-compression failure is small. LY 2 and LY3 are still shear-compression failure, and the crack load and crack width are similar to the corresponding rectangular beams.

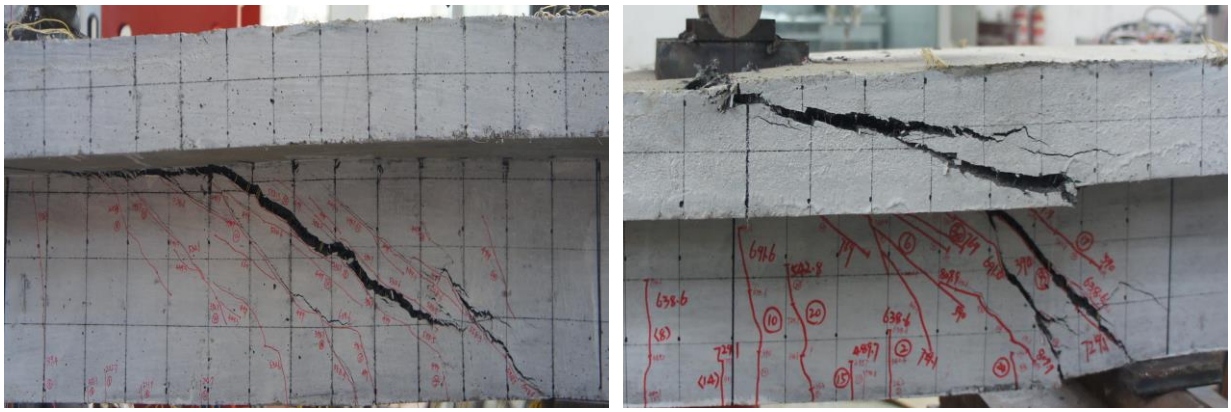

(a) LY1（λ=3.5，ρ_{sv}=0）　　(b) LY2（λ=2.25，ρ_{sv}=0）

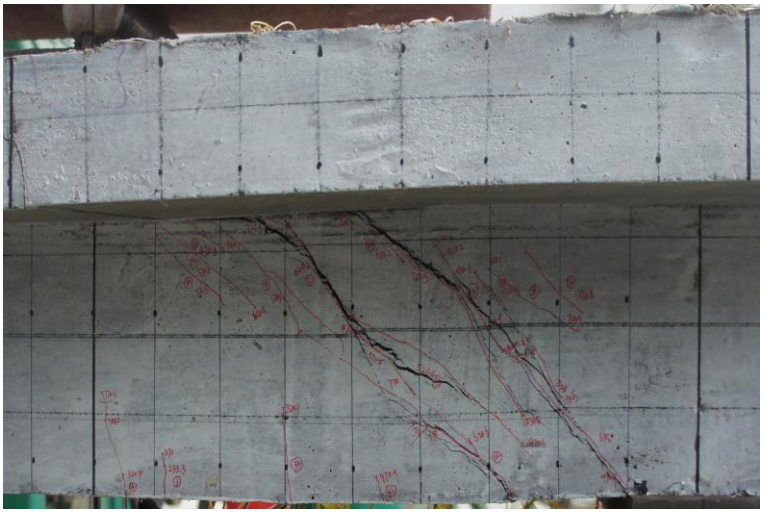

(c) LY3（λ=2.25，ρ_{sv}=0.25%）

Figure 13 Failure mode of RPC beams

Table 9 Test results for RPC beams

	Shape of Section	λ	ρsv/%	Pcr/kN	Pu/kN	wcr/mm	wu/mm	θw/°	Failure mode
LY1	T	3.5	0	319.4	768.8	0.02	10	45	Shear compression
LZ3	R	3.5	0	299	604.1	0.02	5	29	Diagonal Tension
LY2	T	2.25	0	262	1094.5	0.02	10	45	Diagonal Compression
LZ2	R	2.25	0	250.4	901	0.05	10	37	Diagonal Compression
LY3	T	2.25	0.25	290.7	1119.8	0.02	1.22	45	Diagonal Compression
LZ5	R	2.25	0.25	250.8	1005.6	0.02	1.55	37	Diagonal Compression

3.6.2 Shear capacity

It can be seen that the shear capacity of T-shaped beams is obviously improved. Compared with LZ3, LY 2, LZ2, LY3 and LZ5 under the same conditions, the shear capacity of T-shaped beams increases by 27.1%, 21.5% and 15.9% respectively.

3.7 Effect of Angle of stirrups

The test results and failure modes are shown in Figure 14 and Table 10.

3.7.1 Failure mode

The angle of stirrup configuration has little effect on failure mode. The test beams with different angles of stirrup configuration are all shear-compression failure, and the maximum width of oblique crack is similar, but the inclination angle of main oblique crack decreases

with the decrease of angle.

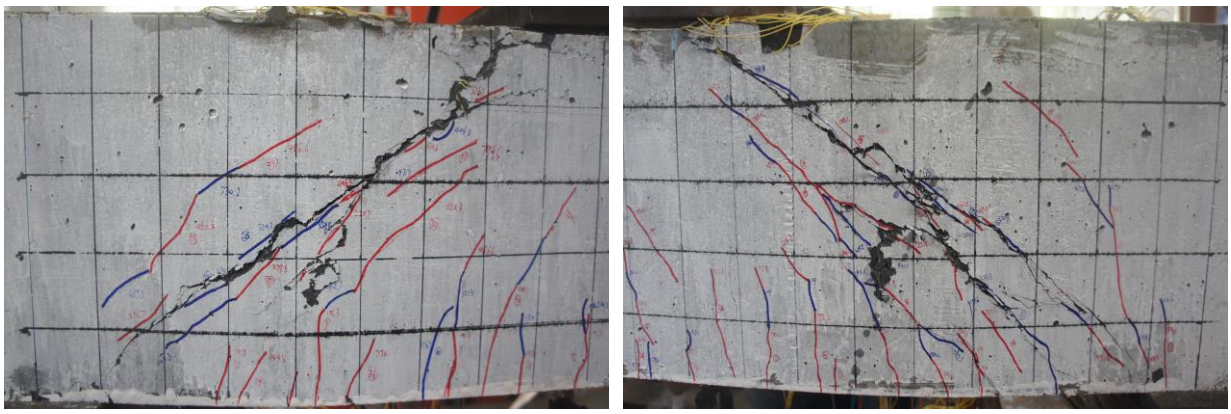

(a) LM1(θ_{sv}=75°)　　(b)LM2(θ_{sv}=60°)

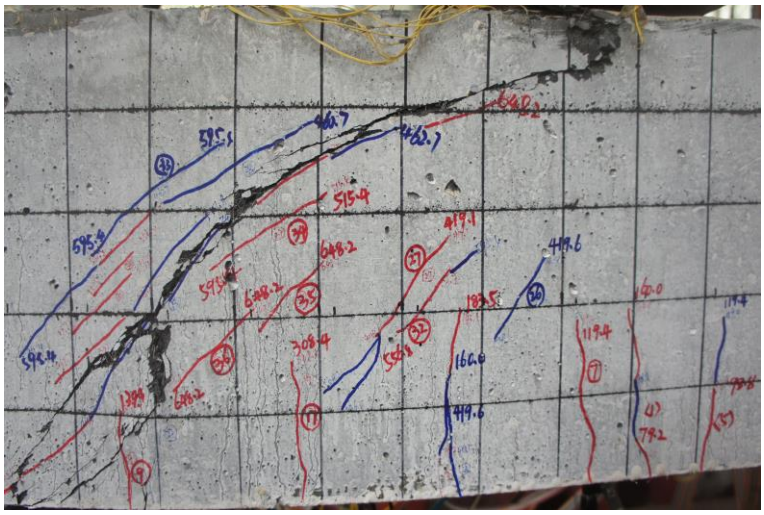

(c)LM3(θ_{sv}=45°)

Figure 14 Failure mode of RPC beams

Table 10 Test results for RPC beams

	θ_{sv}/	P_{cr}/kN	P_u/kN	w_{cr}/mm	w_u/mm	θ_w/°	Failure mode
LM1	75	198.2	879.4	0.01	2.8	42	Diagonal Compression
LM2	60	194.8	901	0.01	4	37	Diagonal Compression
LM3	45	183.5	925	0.02	3	32	Diagonal Compression

3.7.2 Shear capacity

As it shown in Figure 14. It can be found that the angle of stirrups in RPC beams has certain influence on shear capacity. With the increase of stirrup angle, the shear capacity decreases

gradually. When the angle increases from 45 to 60 degrees, the shear capacity decreases by 2.5%, and when the angle increases from 60 to 75 degrees, the shear capacity decreases by 2.7%. However, compared with other parameters, the stirrup angle has little effect on the overall variation of RPC shear capacity.

3.8 Test result analysis

Compared with ordinary concrete beams, the shear capacity of HRC reinforced RPC beams is higher. The shear-compression failure of the test beam is still caused by the early inclined cracks, and the stirrups yield during the failure, but the RPC in the compression zone is not crushed at the end of the failure, with the steel fibers being pulled out at the cracks. It can be seen that, different have different effects on shear capacity:

3.8.1 Effect of Shear span ratio

The shear-span ratio has a great influence on the shear capacity, especially in the absence of web reinforcement, the influence of shear-span ratio is more significant, and the influence of the shear-span ratio on the shear capacity of beams with web reinforcement is reduced. The smaller the shear span ratio is, the higher the shear capacity is. The shear span ratio has the greatest influence on the shear capacity in the range of 1.5-2.25 (50.7% increase in shear span ratio). The shear capacity of beams without web reinforcement decreases by 55.45% on average, and the shear capacity of beams with web reinforcement decreases by 28.35% on average. Then the influence of shear span ratio on shear capacity decreases and tends to be flat. At the same time, it can be seen from the experimental phenomena that the shear span ratio determines the failure mode of the test beam to a great extent.

3.8.2 Effect of Longitudinal reinforcement ratio

There is a linear relationship between the longitudinal reinforcement ratio and the shear capacity. The longitudinal reinforcement ratio of beams without web reinforcement increases from 4.48% to 8.18% (82.6%) and the shear capacity increases by 49.9%. The longitudinal reinforcement ratio of beams with web reinforcement increased from 6.58% to 9.87% (up 50%) and the shear capacity increased by 26.8% on average. When the longitudinal reinforcement ratio exceeds 8.18%, the benefit of shear capacity will not increase. In addition, the test results show that the longitudinal reinforcement ratio has a certain impact on the failure mode of the beam. When the longitudinal reinforcement ratio is allocated more,

the test beam shows the properties of diagonal compression failure.

In the shear failure test, the longitudinal bars also restrain the development of inclined cracks in the shear span area. In addition, longitudinal reinforcement can balance the compressive stress of RPC in compression zone, so that the height of compression zone can be raised, thereby improving the shear capacity. In addition, because of its super-high strength, the limit reinforcement ratio of RPC beams is as high as 10%. Therefore, the longitudinal reinforcement can improve the shear capacity effectively. However, the longitudinal reinforcement restricts the rotation of members, so when the longitudinal reinforcement ratio is high, the ductility of members decreases, and the failure of beam web changes from shear dislocation to compression shear failure of RPC, forming a crack zone, and the destructive nature of members tends to baroclinic failure.

3.8.3 Effect of Stirrup ratio

From the test results, it can be seen that the increase of shear capacity is 21.0% during the period of increasing stirrup ratio from 0 to 0.25%. The maximum increase is 11.6% with the increase of longitudinal reinforcement ratio and 17.9% with the increase of shear span ratio. According to the test results, the stirrup ratio can only increase the shear capacity in a certain range, and the maximum benefit can be achieved when the stirrup ratio is 0.25%. With the increase of the stirrup ratio, the growth rate will also decrease. With the increase of stirrup ratio, the stirrup density in shear span area increases, and the restriction on RPC increases, so the shear capacity of members increases. In addition, the smaller the spacing of stirrups, the better the effect of stirrups, and the lower the width of diagonal cracks. With the increase of stirrup ratio, the failure mode of beams with high shear span ratio is improved from tension diagonal failure without web reinforcement to shear-compression failure. When the stirrup ratio is too high, the shear capacity of the test beam is far greater than the flexural capacity, which is prone to bending failure.

3.8.4 Effect of Horizontal web reinforcement ratio

When the reinforcement ratio of horizontal web reinforcement increases from 0.25% to 0.76%, the shear capacity increases by 29.1%. When the ratio of horizontal web reinforcement reaches 0.51%, the increase of shear capacity decreases. It can be seen from the test that the shear capacity of beams with web reinforcement can be improved by increasing the ratio of horizontal web reinforcement, but the increase of shear capacity of

horizontal web reinforcement is less than that of stirrups under the same ratio of reinforcement. The increase of reinforcement ratio of horizontal web reinforcement does not affect the change of failure mode, but with the increase of reinforcement ratio of horizontal web reinforcement, the crack width increases, and the inclination angle increases gradually.

Horizontal web reinforcement plays the same role as longitudinal reinforcement. Because high-strength reinforced RPC beams often have shear inclined cracks, adding horizontal web reinforcement can effectively restrain the development of inclined cracks and reduce the width of cracks. The strength of horizontal web reinforcement used in this experiment is low, and the actual results have not reached the desired state, which needs to be further studied.

3.8.5 Effect of Dosage of steel fibers

According to the test results of the influence of steel fibers, the content of steel fibers directly affects the shear capacity of RPC. The volume ratio of steel fibers increases from 0 to 3%, and the shear capacity increases by 257.4%. From the mechanical energy, it can be seen that the compressive and tensile strength of RPC increases with the increase of steel fiber volume fraction, reaching the maximum benefit at 2%, while the shear test of the test beam has the same results. When steel fibers are added, the member changes from cable-stayed failure to shear-compression failure. It can be seen that steel fibers have an important contribution to the failure mode of beams.

For the test beams without steel fibers cracks develop rapidly until they are damaged under load. After the cracks occur, the steel fibers between the cracks can play the role of bridge, restrain the crack development, until the steel fibers are fully pulled out before losing effect, and then the components are damaged, so the ductility of the components has been greatly improved. The shear capacity of test beams with steel fibers is higher. When more steel fibers are added, it is easy to agglomerate steel fibers, which cannot be tied with cementitious materials.

3.8.6 Effect of Section shape

The change of section shape makes the shear capacity of T-beam higher than that of rectangular beam. Under the influence of different parameters, the section shape increases the shear capacity by an average of 21.5%. When the parameters change, the growth and decay trend of T-beam is the same as that of rectangular beam. The cracking load and ultimate load of T-beam are larger than rectangular beam, but the width of main diagonal

crack is similar under shear-compression failure. When the shear span is large, the failure mode of T-beam is changed from cable-stayed to shear-compression, that is to say, the failure mode of T-beam is improved.

Similar to ordinary concrete beams, in reactive powder concrete, the flange increases the area of RPC in the shear-compression zone of test beams, decreases the height of compression zone, and can bear certain tensile stress, delays the development of cracks, enhances the shear capacity and improves the failure mode.

3.8.7 Effect of Angle of stirrup arrangement

Similar to ordinary concrete, the shear capacity decreases with the increase of stirrup angle. When the stirrup angle increases from 45 to 75 degrees, the shear capacity decreases by 5.2%, which shows that the decrease is small. The angle of stirrup configuration has little effect on the failure mode.

The test beam is subjected to bending and shearing at the shear span under concentrated load. Diagonal cracks are prone to occur at the loading point and the support. The test beam is destroyed along the development position of the oblique cracks in the web, and the inclination angle of the main oblique crack is 45 degrees. The inclined stirrups in the shear span are arranged vertically with the inclined cracks at 45 degrees, even if they are in accordance with the direction of the principal tensile stress, so that the stirrups can play a maximum role in restraining the development of the inclined cracks. At the same time, the inclined stirrups make the area of the shear-compression zone increase and increase the shear bearing capacity.

3.9 Variance analysis of test results

Because the unit of parameters and the magnitude e of increase are different, this paper uses variance analysis method to analyze the influence of the parameters. Only one parameter of test beam is selected to solve the standard deviation.

Table 11 results of variance analysis

	λ	ρ_f	ρ_s	Shape of section	ρ_{sv}	ρ_{sh}	θ_{sv}
Standard deviation	179.86	167.93	151.68	136.83	80.11	53.03	22.81

Based on the comprehensive test results and the results of variance analysis in Table 11, it can be seen that for the high-strength reinforcement RPC, the influence of shear-span ratio, steel fiber volume ratio, longitudinal reinforcement ratio, section shape, stirrup ratio, horizontal web reinforcement ratio and stirrup angle on Shear capacity are ranked from large to small in the order of shear-span ratio, steel fiber volume ratio, longitudinal reinforcement ratio, section shape, stirrup ratio, horizontal web reinforcement ratio and stirrup angle. Therefore, in the companion Cao et al. (2019), the main parameters to be considered for thermotical investigation are shear span ratio, longitudinal reinforcement ratio, stirrup ratio, steel fibre volume ratio and section shape.

4. Conclusion

In this paper, 32 shear tests have been performed to investigate the shear capacity and failure mode of HSR reinforced RPC concrete. Below conclusion can be obtained:

1. Compared with ordinary concrete beams, the HSR reinforced RPC beam exhibits higher shear capacity.
2. The addition of steel fibre is important in this new type of beams. The steel fibre content directly affects the shear capacity of RPC, and we suggest its optimal dosage to be 2%.
3. The web reinforcement is also recommended in this new type structure, they can effectively restrain the core concrete, reduce the shear stress near the neutral axis, and cracks
4. Through shear tests and variance analysis, the influence of different parameters on the behaviour of this type of structures have been identified. The degree of influence from large to small in order is: Shear span-to-effective depth ratio, volume ratio of steel fiber, longitudinal reinforcement ratio, section shape, stirrup reinforcement ratio, horizontal web reinforcement ratio, stirrups configuration angle.

Acknowledgements

This research was financially supported by the National Natural Science Foundation of China (Grant no. 51368013), The authors wish to acknowledge the sponsors. However, any opinions, findings, conclusions and recommendations presented in this paper are those of the authors and do not necessarily reflect the views of the sponsors.

Reference

Aitcin P.C, “Cements of yesterday and today Concrete of tomorrow”, Cement and Concrete Research, Vol. 30, (2000), pp 1349 - 1359.

Basu P.C, “Performance Requirements of HPC for Indian NPP Structures”, The Indian Concrete Journal, Sep. 1999, pp. 539 – 546.

Bonneau O, Vernet C, Moranville M, and Aitcin P. C, “Characterization of the granular packing and percolation threshold of reactive powder concrete”, Cement and Concrete Research, Vol. 30 (2000) pp. 1861 – 1867.

Dauriac C, “Special Concrete may give steel stiff competition, Building with Cincrete”, The Seattle Daily Journal of Commerce, May 9, 1997.

Deng Z.C., Chen C.S., Chen X.W. (2015) Experimental study on shear behavior of Hybrid Fiber Reinforced Reactive Powder Concrete Beams, Journal of Civil Engineering, 2015, 48 (05): 51-60.

Goltermann P, Johansen V, and Palbol L, “Packing of Aggregates: An Alternative Tool to Determine the Optimal Aggregate Mix”, ACI Materials Journal, Sep-Oct. 1997, pp. 435 – 443.

He S.h,.Mosallamb A.S, Fang Z.,Sun X.L.,Su J (2018), Experimental evaluation of shear connectors using reactive powder concrete under natural curing condition, Construction and Building Materials, Volume 191, 10 December 2018, Pages 775-786.

Hou X.M., Abid M., Zheng W.Z., Waqar G. Q. (2017), Evaluation of residual mechanical properties of steel fiber-reinforced reactive powder concrete after exposure to high temperature using nondestructive testing, Procedia Engineering, Volume 210, 2017, Pages 588-596

Jin L.Z., He L., Wu X.H. (2015). Experimental study on flexural behavior of reinforced RPC beams with HRB500 grade reinforcement, Architectural structure, 2015, 45 (15): 87-92.

Li L (2010), The design method of Reactive powder concrete beam. PhD Thesis, Harbin Institute of Technology .

Reactive Powder Concrete, http://www.theconcreteportal.com/reac_pow.html, last viewed 02/2019

Richard P, and Cheyrezy M, “Composition of Reactive Powder Concrete”, Cement and Concrete Research, Vol. 25, No.7, (1995), pp. 1501 – 1511.

Ridha, M.M.S. Sarsam K.F., Al-Shaarbaf I. A.S. (2018) Experimental Study and Shear Strength Prediction for Reactive Powder Concrete Beams, Case Studies in Construction Materials 8, pp 434-446

Ruan Y.F., Han B.G., Yu X. Li Z., Wang J.L., Dong S.F, Ou J.P. (2018), Mechanical

behaviors of nano-zirconia reinforced reactive powder concrete under compression and flexure, Construction and Building Materials V162 pp 663-673

Su C.D., Wu Q.H., Weng L., Chang X. (2019) Experimental investigation of mode I fracture features of steel fiber-reinforced reactive powder concrete using semi-circular bend test, Engineering Fracture Mechanics, Engineering Fracture Mechanics, Volume 209, 15 March 2019, Pages 187-199

Sun M.D., Gao R., Chen Y.T., Gao M.C. (2016). Experimental study on bonding behavior of high strength steel bar and reactive powder concrete Journal of Bridge construction, 2016, 46 (06): 18-23.

Voo Y L, Stephen J F, RIan G (2006). Shear strength of fiber reinforced reactive powder concrete prestressed girders without stirrups, Journal of Advanced Concrete Technology, 2006,4(1): 123-132.

Voo Y L, Wai K, Stephen J. (2010), Shear strength of steel fiber-reinforced ultrahigh-performance concrete beams without stirrups, Journal of Structure Engineering, 2010, (4): 1393-1399.

Wang Q.W., Shi Q.X., Lui E.M., Xu Z.D. (2019),Axial compressive behavior of reactive powder concrete-filled circular steel tube stub columns, Journal of Constructional Steel Research, Volume 153, February 2019, Pages 42-54.

Xu H.B., Deng Z.C., Chen C.S., Chen X.W. (2014) Experimental study on shear behavior of ultra-high-performance fiber reinforced concrete beams. Journal of Civil Engineering, 2014, 47 (12): 91-97.

Yu T. Hadi M.N. S., Goaiz H.A. (2018), Experimental investigation of CFRP confined hollow core Reactive Powder Concrete columns, Construction and Building Materials, Volume 174, 20 June 2018, Pages 343-355.